

Sum Rate of Two-Way MIMO AF Relay Networks With Transmit/Receive Zero-Forcing

Gayan Amarasuriya, Chintha Tellambura and Masoud Ardakani

Department of Electrical and Computer Engineering, University of Alberta, Edmonton, AB, Canada T6G 2V4

Email: {amarasur, chintha, ardakani}@ece.ualberta.ca

Abstract—The sum rate of multiple-input multiple-output (MIMO) amplify-and-forward (AF) two-way relay networks (TWRNs) with transmit/receive zero-forcing (ZF) is analytically studied. Specifically, the exact sum rate expressions are derived for uncorrelated and semi-correlated Rayleigh fading cases in closed-form. Moreover, the closed-form upper and lower bounds of the sum rate are derived for doubly-correlated Rayleigh fading. In particular, these sum rate bounds are tight, and consequently, serve as benchmarks providing valuable insights into practical MIMO AF TWRN system-design. All the analyses are verified by using Monte-Carlo simulations.

I. INTRODUCTION

Two-way relay networks (TWRNs) are widely considered as the next evolution of conventional one-way relay networks (OWRNs) as the former promises significant spectral efficiency improvements over the latter in the context of wireless networks with half-duplex terminals [1]–[4]. Thus, the forth-generation and subsequent wireless standards are expected to be equipped with this emerging cooperative two-way relay technology. Specifically, multiple-input multiple-output (MIMO) transmission schemes for TWRNs are currently receiving significant research attention as they can significantly improve the performance of single-antenna TWRNs [5]–[7]. In this context, in [8], a novel transmit/receive (Tx/Rx) zero-forcing (ZF) based transmission strategy has recently been proposed and analyzed for MIMO amplify-and-forward (AF) TWRNs. In this paper, the achievable sum rate of MIMO AF TWRNs with Tx/Rx ZF is analytically studied.

Prior related research: The sum rate bounds are derived for the single-antenna AF TWRNs in [1]–[4]. In [1], [2], the sum rate is analytically quantified to verify that TWRNs are twice as spectrum efficient as OWRNs. In [3], the sum rate upper bounds are derived to compare the performance of two time-slot and three time-slot TWRNs with physical layer network coding. Reference [4] studies the sum rate of distributed relay selection strategies for TWRNs.

References [5]–[7], [9] study the sum rate of MIMO AF TWRNs. In particular, [5] studies the achievable sum rate regions by deriving the optimal relay beamforming structures. In [6], the sum-rate is derived for multi-relay TWRNs with optimal relay precoders. Reference [7] quantifies the detrimental impact of channel estimation errors on the sum rate of MIMO TWRN models proposed in [5], [6]. Furthermore, [9] studies the achievable rate regions of MIMO multi-relay AF TWRNs.

Motivation and our contribution: The MIMO TWRN transmission schemes proposed in [5]–[7], [9] employ complicated precoder/decoder designs, and consequently, undermine one of the key trade-offs of designing practical relay networks;

i.e., the implementation complexity versus performance. To be more specific, the practical implementation of transceiver structures of [5]–[7], [9] requires global channel state information (CSI)¹, and hence, results in increased feedback/overhead and reduced spectral efficiencies. Recently, in [8], we proposed and analyzed a suboptimal yet simple Tx/Rx ZF based transmission strategy, which improves the trade-off between implementation complexity and performance of MIMO AF TWRNs. In this paper, the achievable sum rate of this transmission strategy is studied.

Specifically, the exact sum-rate is derived for (i) independent and identically distributed (i.i.d.) Rayleigh fading and (ii) semi-correlated² Rayleigh fading cases. Moreover, tight upper and lower bounds of the sum rate are derived in closed-form for doubly-correlated³ Rayleigh fading. In particular, these sum rate bounds are tight, and hence, serves as useful benchmarks for the exact sum rate. Specifically, our analysis renders themselves useful to analytically quantify the detrimental impact of spatially-correlated fading on the sum rate. Furthermore, numerical results are provided to obtain valuable insights into practical MIMO TWRN implementation.

Notations: \mathbf{I}_n and $\mathbf{0}_{n \times m}$ denote the $n \times n$ identity matrix and $n \times m$ all zero matrix, respectively. \mathbf{Z}^H and \mathbf{Z}^T are the Hermitian transpose and transpose of \mathbf{Z} , respectively. The (i, j) th element of \mathbf{Z} is denoted as $[\mathbf{Z}]_{i,j}$. \mathbf{Z}_i and $\mathbf{Z}_{i,j}$ are the residue matrices resulted from removing the i th column, and i th column and j th row of \mathbf{Z} , respectively. $\mathbf{H} \sim \mathcal{CN}(\mathbf{M}, \mathbf{\Sigma})$ denotes a circular symmetric Gaussian random matrix with mean \mathbf{M} and covariance $\mathbf{\Sigma}$. $\det(\mathbf{Z})$ and \otimes denote the determinant of \mathbf{Z} and the Kronecker product, respectively. $\mathcal{E}_\Lambda\{z\}$ is the expectation of z over Λ . $\psi(x)$ and $\Gamma(a, x)$ are the Euler's digamma function [10, Eq. (8.360.1)] and the upper incomplete Gamma function [10, Eq. (8.350.2)].

II. SYSTEM, CHANNEL AND SIGNAL MODEL

A. System model

We consider a half-duplex MIMO AF TWRN with two sources (S_1 and S_2), and one relay (R), where each equipped with N_1 , N_2 and N_R antennas, respectively. In particular, N_1 , N_2 and N_R are restricted to satisfy the constraint $N_R < \min(N_1, N_2)$ in the sequel. This constraint not only enables us

¹Here, global CSI refers to instantaneous full channel knowledge of both hops, i.e., $S_1 \rightarrow R$ and $S_2 \rightarrow R$.

²The semi-correlated fading is defined as uncorrelated fading at the two sources and arbitrarily-correlated fading at the relay.

³The doubly-correlated fading is defined as arbitrarily-correlated fading at the two sources and relay.

to employ joint transmit/receive ZF for the same antenna setup but also renders mathematical tractability. In this context, the maximum number of end-to-end (e2e) data subchannels is constrained to N_R .

B. Channel model

The channel matrix from S_i to R is denoted by $\mathbf{H}^{(i,R)} \in \mathbb{C}^{N_R \times N_i}$ for $i \in \{1, 2\}$. All the channel fading amplitudes are assumed to be remain fixed over two consecutive time-slots [1], [3], and consequently, the channel matrix from R to S_i , $\mathbf{H}^{(R,i)} \in \mathbb{C}^{N_i \times N_R}$, can be denoted as $(\mathbf{H}^{(i,R)})^T$ for $i \in \{1, 2\}$. The direct channel between S_1 and S_2 is assumed to be unavailable due to heavy path-loss and shadowing [1], [3]. All channel amplitudes are assumed to be distributed as frequency-flat Rayleigh fading as follows:

1) *Uncorrelated Rayleigh fading*: Assuming a rich scattering scenario, no line-of-sight path, and larger relative antenna spacing and angular spreads, the channel matrix between S_i and R can be written as [11]

$$\mathbf{H}^{(R,i)} = \mathbf{H}^{(i)} \sim \mathcal{CN}(\mathbf{0}_{N_i \times N_R}, \mathbf{I}_{N_i} \otimes \mathbf{I}_{N_R}) \text{ for } i \in \{1, 2\}. \quad (1)$$

2) *Semi-correlated Rayleigh fading*: Assuming limited relative antenna spacing and angular spreads at R , the fading channel matrix between S_i and R can be written as [11]

$$\mathbf{H}^{(R,i)} = \mathbf{H}^{(i)} \left(\Psi^{(R,i)} \right)^{\frac{1}{2}} \text{ for } i \in \{1, 2\}, \quad (2)$$

where $\Psi^{(R,i)} \in \mathbb{C}^{N_R \times N_R}$ is the Hermitian and positive definite correlation matrix at R . Thus, $\mathbf{H}^{(R,i)}$ is denoted as $\mathbf{H}^{(R,i)} \sim \mathcal{CN}(\mathbf{0}_{N_i \times N_R}, \mathbf{I}_{N_i} \otimes \Psi^{(R,i)})$ for $i \in \{1, 2\}$.

3) *Doubly-correlated Rayleigh fading*: Assuming limited relative antenna spacing and angular spreads at both sources and the relay, the fading channel matrix between S_i and R can be written as [11]

$$\mathbf{H}^{(R,i)} = \left(\Phi^{(R,i)} \right)^{\frac{1}{2}} \mathbf{H}^{(i)} \left(\Psi^{(R,i)} \right)^{\frac{1}{2}} \text{ for } i \in \{1, 2\}, \quad (3)$$

where $\Phi^{(R,i)} \in \mathbb{C}^{N_i \times N_i}$ and $\Psi^{(R,i)} \in \mathbb{C}^{N_R \times N_R}$ are the Hermitian and positive definite correlation matrices at the source and relay, respectively. Thus, $\mathbf{H}^{(R,i)}$ is denoted as $\mathbf{H}^{(R,i)} \sim \mathcal{CN}(\mathbf{0}_{N_i \times N_R}, \Phi^{(R,i)} \otimes \Psi^{(R,i)})$ for $i \in \{1, 2\}$.

C. Signal model

During the first time-slot, S_1 and S_2 transmit \mathbf{x}_1 and \mathbf{x}_2 simultaneously by employing transmit-ZF precoding to R over a multiple access channel. These information-bearing vectors satisfy $\mathcal{E}[\mathbf{x}_i \mathbf{x}_i^H] = \mathbf{I}_{N_i}$ for $i \in \{1, 2\}$. The received superimposed-signal vector or the analog network code vector at R is given by

$$\mathbf{y}_R = g_1 \mathbf{H}^{(1,R)} \mathbf{F}_1 \mathbf{x}_1 + g_2 \mathbf{H}^{(2,R)} \mathbf{F}_2 \mathbf{x}_2 + \mathbf{n}_R, \quad (4)$$

where \mathbf{n}_R is the $N_R \times 1$ zero mean Gaussian noise vector at R satisfying $\mathcal{E}(\mathbf{n}_R \mathbf{n}_R^H) = \mathbf{I}_{N_R} \sigma_R^2$, and \mathbf{F}_i is the transmit-ZF precoding matrix at S_i , and is given by [12]

$$\mathbf{F}_i = \left(\mathbf{H}^{(i,R)} \right)^H \left(\mathbf{H}^{(i,R)} \left(\mathbf{H}^{(i,R)} \right)^H \right)^{-1} \Pi_i \text{ for } i \in \{1, 2\}, \quad (5)$$

where Π_i is the $N_R \times N_i$ permutation matrix⁴ constructed to ensure only N_R data streams are transmitted by S_i for $i \in \{1, 2\}$. In (5), g_i , $i \in \{1, 2\}$, is the power normalizing factor designed to constraint the long-term total power at S_i as

$$g_i = \sqrt{\frac{\mathcal{P}_i}{\text{Tr}(\mathcal{E}[\mathbf{F}_i \mathbf{F}_i^H])}} = \sqrt{\frac{\mathcal{P}_i}{\mathcal{T}_i}}, \text{ for } i \in \{1, 2\}, \quad (6)$$

where $\mathcal{T}_i \triangleq \text{Tr}(\mathcal{E}[\mathbf{F}_i \mathbf{F}_i^H]) = \frac{N_R}{N_i - N_R}$ [13] and \mathcal{P}_i is the transmit power at S_i for $i \in \{1, 2\}$.

During the second time slot, R amplifies \mathbf{y}_R with a gain⁵ $G = \sqrt{\mathcal{P}_R / (g_1^2 + g_2^2 + \sigma_R^2)}$ and transmits back to both sources over the broadcast channel. Here, \mathcal{P}_R is the transmit power at R . Then, each source receives the $N_R \times 1$ signal vector by employing the receive-ZF reconstruction matrix as follows:

$$\mathbf{y}_{S_i} = \mathbf{W}_i \left(G \mathbf{H}^{(R,i)} \mathbf{y}_R + \mathbf{n}_i \right), \text{ for } i \in \{1, 2\}, \quad (7)$$

where $\mathbf{H}^{(R,i)} = (\mathbf{H}^{(i,R)})^T$ and \mathbf{n}_i is the $N_i \times 1$ zero mean Gaussian noise vector at S_i satisfying $\mathcal{E}(\mathbf{n}_i \mathbf{n}_i^H) = \mathbf{I}_{N_i} \sigma_i^2$ for $i \in \{1, 2\}$. In (7), \mathbf{W}_i , $i \in \{1, 2\}$, is the receive-ZF reconstruction matrix at S_i , and given by [12]

$$\mathbf{W}_i = \left(\left(\mathbf{H}^{(R,i)} \right)^H \mathbf{H}^{(R,i)} \right)^{-1} \left(\mathbf{H}^{(R,i)} \right)^H, \text{ for } i \in \{1, 2\}. \quad (8)$$

By substituting (4) and (8) into (7), and by removing the self-interference⁶ [1], the post-processing end-to-end signal-to-noise ratio (e2e SNR) of the k th, $k \in \{1 \cdots N_R\}$, data subchannel at S_i can be derived as in (9). In (9), $\tilde{\gamma}_{i,R} \triangleq \frac{\mathcal{P}_i}{\sigma_R^2}$, $\tilde{\gamma}_{R,i} \triangleq \frac{\mathcal{P}_R}{\sigma_i^2}$, $i \in \{1, 2\}$, $i' \in \{1, 2\}$ and $i \neq i'$. It is worth noticing the statistical independence of $\gamma_{S_1^{(k)}}$ and $\gamma_{S_2^{(k)}}$ of (9) for a given k . However, the post-processing SNRs of multiple subchannels belong to a given source are correlated. Nevertheless, by employing the simple detection scheme in [14], [15], the corresponding symbols of each antenna can be independently decoded. Thus the achievable sum rate assuming independent decoding at both S_1 and S_2 can be written as the sum of rates of all subchannels as [14]–[16]

$$\mathcal{C} = \frac{1}{2} \sum_{i=1}^2 \sum_{k=1}^{N_R} \mathcal{E} \left\{ \log_2 \left(1 + \gamma_{S_i^{(k)}} \right) \right\}. \quad (10)$$

III. SUM RATE ANALYSIS OF MIMO AF TWRNs

In this section, the sum rate of MIMO AF TWRNs with Tx/Rx ZF is analytically quantified. To this end, the exact sum rate expressions for uncorrelated Rayleigh fading and arbitrarily semi-correlated Rayleigh fading are derived in closed-form. Moreover, tight upper and lower bounds of the sum rate are derived for arbitrarily doubly-correlated Rayleigh fading.

⁴The permutation matrix, Π_i , $i \in \{1, 2\}$, can be constructed by horizontally concatenating a $N_R \times N_R$ permutation matrix and a $N_R \times (N_i - N_R)$ zero matrix [8].

⁵This amplification factor, G , is designed as a normalizing constant to constraint the long-term total power at R [8].

⁶It is assumed that S_i knows its own information-bearing symbol vector, \mathbf{x}_i , CSI of $\mathbf{H}_{i,R}$, and G which requires Ψ_i , where $i \in \{1, 2\}$.

$$\gamma_{S_i^{(k)}} = \frac{\mathcal{T}_i \bar{\gamma}_{R,i} \bar{\gamma}_{i',R}}{\mathcal{T}_i \mathcal{T}_{i'} \bar{\gamma}_{R,i} + (\mathcal{T}_i \bar{\gamma}_{i',R} + \mathcal{T}_{i'} \bar{\gamma}_{i,R} + \mathcal{T}_i \mathcal{T}_{i'}) \left[\left(\mathbf{H}^{(R,i)} \right)^H \mathbf{H}^{(R,i)} \right]^{-1}_{k,k}}, \text{ for } k \in \{1, \dots, N_R\}, i \in \{1, 2\}, i' \in \{1, 2\} \text{ and } i \neq i'. \quad (9)$$

$$\mathcal{C} \leq \mathcal{C}_{ub} = \frac{1}{2 \ln(2)} \sum_{i=1}^2 \sum_{k=1}^{N_R} \ln \left[\frac{(\zeta_i + \eta_i) (N_R)! \det(\mathcal{A}^{(i)}) \prod_{u < v}^{N_i-1} (\tau_{v,kk}^{(i)} - \tau_{u,kk}^{(i)}) + \mu \phi_{i,k} (N_R - 1)! \det(\mathcal{A}_{kk}^{(i)}) \prod_{p < q}^{N_i} (\tau_q^{(i)} - \tau_p^{(i)})}{\zeta_i (N_R)! \det(\mathcal{A}^{(i)}) \prod_{u < v}^{N_i-1} (\tau_{v,kk}^{(i)} - \tau_{u,kk}^{(i)}) + \mu \phi_{i,k} (N_R - 1)! \det(\mathcal{A}_{kk}^{(i)}) \prod_{p < q}^{N_i} (\tau_q^{(i)} - \tau_p^{(i)})} \right]. \quad (14)$$

$$\mathcal{C} \geq \mathcal{C}_{lb} = \frac{1}{2 \ln(2)} \sum_{i=1}^2 \sum_{k=1}^{N_R} \ln \left[1 + \frac{\eta_i \prod_{p < q}^{N_i} (\tau_q^{(i)} - \tau_p^{(i)}) \prod_{u < v}^{N_i-1} (\tau_{v,kk}^{(i)} - \tau_{u,kk}^{(i)}) \exp \left(\sum_{l=1}^{N_R} \psi(l) + \left(\prod_{p < q}^{N_i} (\tau_q^{(i)} - \tau_p^{(i)}) \right)^{-1} \sum_{l=N_i-N_R+1}^{N_i} \det(\mathcal{B}^{(i,k)}) \right)}{\zeta_i (N_R)! \det(\mathcal{A}^{(i)}) \prod_{u < v}^{N_i-1} (\tau_{v,kk}^{(i)} - \tau_{u,kk}^{(i)}) + \mu \phi_{i,k} (N_R - 1)! \det(\mathcal{A}_{kk}^{(i)}) \prod_{p < q}^{N_i} (\tau_q^{(i)} - \tau_p^{(i)})} \right]. \quad (17)$$

A. Uncorrelated Rayleigh fading

The sum rate of MIMO AF TWRNs with Tx/Rx ZF over i.i.d. Rayleigh fading is derived as (see Appendix I for the proof)

$$\mathcal{C} = \frac{N_R}{2 \ln(2)} \sum_{i=1}^2 [\mathbb{J}(N_i - N_R, \mu, \eta_i + \zeta_i) - \mathbb{J}(N_i - N_R, \mu, \zeta_i)], \quad (11)$$

where the function $\mathbb{J}(\cdot, \cdot, \cdot)$ in (11) is defined as

$$\mathbb{J}(a, b, c) = \ln(b) + \exp\left(\frac{b}{c}\right) \sum_{m=0}^a \sum_{n=0}^m \frac{\binom{m}{n} (-b)^{m-n} \Gamma(n, \frac{b}{c})}{(m)! c^{m-n}}. \quad (12)$$

Moreover, $\mu = \mathcal{T}_1 \bar{\gamma}_{S_2 R} + \mathcal{T}_2 \bar{\gamma}_{S_1 R} + \mathcal{T}_1 \mathcal{T}_2$, $\eta_1 = \mathcal{T}_1 \bar{\gamma}_{R S_1} \bar{\gamma}_{S_2 R}$, $\eta_2 = \mathcal{T}_2 \bar{\gamma}_{R S_2} \bar{\gamma}_{S_1 R}$, $\zeta_1 = \mathcal{T}_1 \mathcal{T}_2 \bar{\gamma}_{R S_1}$, and $\zeta_2 = \mathcal{T}_1 \mathcal{T}_2 \bar{\gamma}_{R S_2}$.

B. Semi-correlated Rayleigh fading

For arbitrarily correlated antennas at R and uncorrelated antennas at S_i , where $i \in \{1, 2\}$, the sum rate of MIMO AF TWRNs with Tx/Rx ZF is derived as (see Appendix I for the proof)

$$\mathcal{C} = \frac{1}{2 \ln(2)} \sum_{i=1}^2 \sum_{k=1}^{N_R} [\mathbb{J}(N_i - N_R, \mu \phi_{i,k}, \eta_i + \zeta_i) - \mathbb{J}(N_i - N_R, \mu \phi_{i,k}, \zeta_i)], \quad (13)$$

where $\phi_{i,k}$ for $i \in \{1, 2\}$ and $k \in \{1, \dots, N_R\}$ is the k th diagonal element of $\Psi_{R,i}^{-1}$. Again, the function $\mathbb{J}(\cdot, \cdot, \cdot)$ is defined in (12).

C. Doubly-correlated Rayleigh fading

The exact sum rate of MIMO AF TWRNs with Tx/Rx ZF over doubly-correlated Rayleigh fading appears mathematically intractable. Thus, the upper and lower bounds of the sum rate are derived as follows:

1) *Upper bound*: An upper bound of the sum rate of MIMO AF TWRNs with Tx/Rx ZF over doubly-correlated Rayleigh fading is derived as in (14) (see Appendix II for the proof).

In (14), $\mathcal{A}^{(i)}$ is an $N_i \times N_i$ matrix with (a, b) th entry given by

$$[\mathcal{A}^{(i)}]_{a,b} = \begin{cases} \left(\tau_a^{(i)}\right)^{b-1}, & b = 1, \dots, N_i - N_R \\ \left(\tau_a^{(i)}\right)^b, & b = N_i - N_R + 1, \dots, N_R \end{cases}, \quad (15)$$

where $\tau_a^{(i)}$ for $a \in \{1, \dots, N_i\}$ is the real, positive eigenvalues of receive correlation matrix at S_i denoted by $\Phi^{(i)}$. Similarly, $\mathcal{A}_{kk}^{(i)}$ is an $(N_i - 1) \times (N_i - 1)$ matrix with (a, b) th element given by

$$[\mathcal{A}_{kk}^{(i)}]_{a,b} = \begin{cases} \left(\tau_{a,kk}^{(i)}\right)^{b-1}, & b = 1, \dots, N_i - N_R \\ \left(\tau_{a,kk}^{(i)}\right)^b, & b = N_i - N_R + 1, \dots, N_R \end{cases}, \quad (16)$$

where $\tau_{a,kk}^{(i)}$ for $a \in \{1, \dots, N_i\}$ is the real, positive eigenvalues of $\Phi_{kk}^{(i)}$.

2) *Lower bound*: A lower bound of the sum rate of MIMO AF TWRNs with Tx/Rx ZF over doubly-correlated Rayleigh fading is derived as in (17) (see Appendix III for the proof). In (14), $\mathcal{B}_{i,k}$ is an $N_i \times N_i$ matrix with (a, b) th entry given by

$$[\mathcal{B}^{(i,k)}]_{a,b} = \begin{cases} \left(\tau_a^{(i)}\right)^{b-1}, & b \neq k \\ \left(\tau_a^{(i)}\right)^{b-1} \ln(\tau_a^{(i)}), & b = k \end{cases}. \quad (18)$$

IV. NUMERICAL RESULTS

This section presents the numerical results for the sum rate performance of MIMO AF TWRNs with Tx/Rx ZF.

A. Sum rate over uncorrelated Rayleigh fading

Fig. 1 shows the sum rate of MIMO AF TWRNs over i.i.d. Rayleigh fading. The analytical sum rate curves are plotted by using (11) for several antenna configurations. The sum rate curves corresponding to single-antenna relays are plotted as a benchmark. Our results reveals that the number of antennas at the relay directly determines the achievable spatial multiplexing gain. For example, at the average transmit SNR

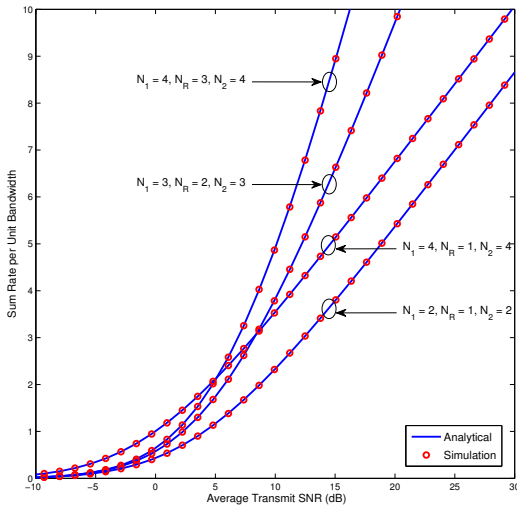


Fig. 1. The sum rate of a MIMO AF TWRN with Tx/Rx ZF over i.i.d. Rayleigh fading.

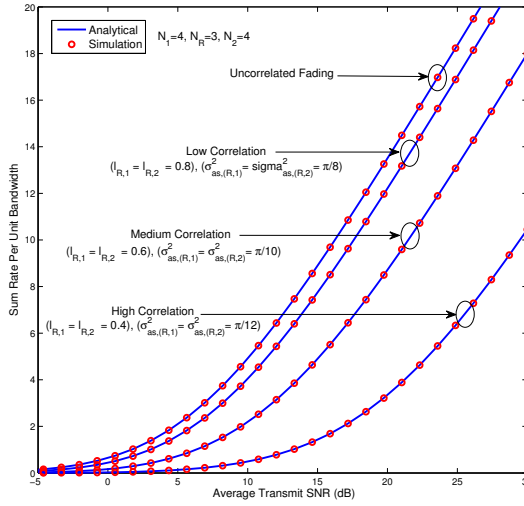


Fig. 2. The sum rate of a MIMO AF TWRN with Tx/Rx ZF over semi-correlated Rayleigh fading. The angle of arrival/departure is given by $\theta_{R,i} = \bar{\theta}_{R,i} + \hat{\theta}_{R,i}$ with $\hat{\theta}_{R,i} \sim \mathcal{N}(0, \sigma_{a.s.}^2(R,i))$, where $\bar{\theta}_{R,i} = \pi/6$ for $i \in \{1, 2\}$.

of 15 dB, the triple-antenna relay corresponding to the TWRN with $N_i|_{i=1}^2 = 4$ antenna set-up achieves approximately two-fold capacity improvement compared to its single-antenna relay counterpart. The exact match between the analytical and simulation points validates our analysis.

B. Sum rate over semi-correlated Rayleigh fading

In Fig. 2, the sum rate is plotted over semi-correlated Rayleigh fading (i.e., spatially-correlated fading at the relay only). The correlation matrices at the relay, $\Psi^{(R,i)}$ for $i \in \{1, 2\}$, is constructed by employing the practical MIMO channel model in [17]⁷. Three different correlation scenarios

⁷The (p, q) th element of $\Psi^{(R,i)}$ for $i \in \{1, 2\}$ is constructed as [17] $[\Psi^{(R,i)}]_{p,q} = e^{-j2\pi(p-q)l_{R,i} \cos(\bar{\theta}_{R,i})} e^{-\frac{1}{2}(2\pi(p-q)l_{R,i} \sin(\bar{\theta}_{R,i}) \sigma_{a.s.}(R,i))^2}$, where $l_{R,i}$ is the relative antenna spacing, $\bar{\theta}_{R,i}$ is the mean angle of arrival/departure, and $\sigma_{a.s.}^2(R,i)$ is the angular spread. This correlation model typically arises in practice in uniform linear antenna arrays.

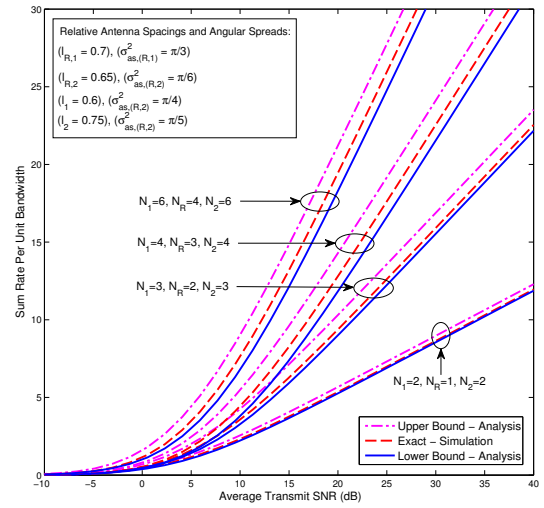


Fig. 3. The sum rate of a MIMO AF TWRN with Tx/Rx ZF over doubly-correlated Rayleigh fading. The angle of arrival/departure is given by $\theta_{R,i} = \bar{\theta}_{R,i} + \hat{\theta}_{R,i}$ with $\hat{\theta}_{R,i} \sim \mathcal{N}(0, \sigma_{a.s.}^2(R,i))$, where $\bar{\theta}_{R,i} = \pi/6$ for $i \in \{1, 2\}$.

are obtained as (a) high correlation, (b) medium correlation, and (c) low correlation. Since $l_{R,i}$ and $\sigma_{a.s.}^2(R,i)$ are the relative antenna spacing and angular spreads, smaller the $l_{R,i}$ and $\sigma_{a.s.}^2(R,i)$, higher the spatial correlation [17]. Our results clearly reveal that correlated fading results in significant sum rate degradation. For example, at a sum rate of 4 bits/second/channel-use, high correlation results in almost 13 dB SNR loss.

C. Sum rate over doubly-correlated Rayleigh fading

In Fig. 3, the sum rate over doubly-correlated Rayleigh fading is plotted for several antenna set-ups. In particular, the upper bound, lower bound and exact sum rate are plotted by using (14), (17), and Monte-Carlo simulations, respectively. The correlation matrices are constructed by again employing the practical MIMO channel model in [17]. Fig. 3 clearly reveals that our analytical bounds are relatively tight specifically for lower number of antennas at each terminal, and hence, provides valuable insights. Thus they render themselves useful as benchmarks for practical TWRN system-designs.

V. CONCLUSION

The sum rate of Tx/Rx ZF based spatial multiplexing transmission strategy for MIMO AF TWRNs is analytically studied. The exact closed-form sum rate expressions are derived for uncorrelated and semi-correlated Rayleigh fading. Moreover, doubly-correlated Rayleigh fading case is treated by deriving closed-form tight upper and lower bounds of the sum rate. Our numerical results reveals that the spatially-correlated fading degrades the sum rate significantly. Our analysis and numerical results provides valuable insights into practical MIMO AF TWRN system-design.

APPENDIX I

Proof of the sum rate for i.i.d. Rayleigh fading and semi-correlated Rayleigh fading

In this Appendix, the proof of the sum rate of MIMO AF TWRNs over semi-correlated Rayleigh fading is first sketched,

and then used to derive the sum rate over i.i.d. Rayleigh fading. To this end, the e2e SNR of the k -th data stream at S_i for $i \in \{1, 2\}$ in (9) can be re-written as

$$\gamma_{S_i^{(k)}} = \frac{\eta_i}{\zeta_i + \mu X_i}, \quad \text{for } i \in \{1, 2\}, \quad (19)$$

where $X_i = \left[\left(\left(\mathbf{H}^{(i,R)} \right)^H \mathbf{H}^{(i,R)} \right)^{-1} \right]_{k,k}$. Here, μ , η_i , and ζ_i are defined in (11). The CDF of $\gamma_{S_i^{(k)}}$ can now be derived as

$$F_{\gamma_{S_i^{(k)}}}(x) = \Pr(\gamma_{S_i^{(k)}} \leq x) = 1 - \Pr\left(X_i \leq \frac{\eta_i - \zeta_i x}{\mu x}\right). \quad (20)$$

For $x \geq \frac{\eta_i}{\zeta_i}$, $F_{\gamma_{S_i^{(k)}}}(x) = 1$, and for $x < \frac{\eta_i}{\zeta_i}$, $F_{\gamma_{S_i^{(k)}}}(x)$ becomes

$$F_{\gamma_{S_i^{(k)}}}(x) = 1 - \int_0^{\frac{\eta_i - \zeta_i x}{\mu x}} f_{X_i}(y) dy. \quad (21)$$

Next, the PDF of $1/X_i$ over semi-correlated Rayleigh fading is given by [14]

$$f_{1/X_i}(x) = \frac{\phi_{i,k}^{N_i - N_R + 1} x^{N_i - N_R} e^{-\phi_{i,k} x}}{\Gamma(N_i - N_R + 1)}, \quad (22)$$

where $\phi_{i,k}$ is the k th diagonal element of $\Psi_{R,i}^{-1}$. The PDF of X can then be derived by substituting (22) into the transformation $f_{X_i}(x) = \frac{1}{x^2} f_{1/X_i}(1/x)$ as follows:

$$f_{X_i}(x) = \frac{\phi_{i,k}^{N_i - N_R + 1} e^{-\phi_{i,k}/x}}{\Gamma(N_i - N_R + 1) x^{N_i - N_R + 2}}. \quad (23)$$

Next, by substituting (23) into (21), and by applying a change of variable, $y = 1/t$, (21) can be rearranged as

$$F_{\gamma_{S_i^{(k)}}}(x) = 1 - \int_{\frac{\mu x}{\eta_i - \zeta_i x}}^{\infty} \frac{\phi_{i,k}^{N_i - N_R + 1} t^{N_i - N_R} e^{-\phi_{i,k} t}}{\Gamma(N_i - N_R + 1)} dt. \quad (24)$$

The PDF of $\gamma_{S_i^{(k)}}$, $f_{\gamma_{S_i^{(k)}}}(x)$, can readily be derived by differentiating (24) with respect to variable x by using the Leibniz integral rule [18] as follows:

$$\begin{aligned} f_{\gamma_{S_i^{(k)}}}(x) &= \frac{\phi_{i,k}^{N_i - N_R + 1} e^{-\frac{\mu \phi_{i,k} x}{\eta_i - \zeta_i x}}}{\Gamma(N_i - N_R + 1)} \left(\frac{\mu x}{\eta_i - \zeta_i x} \right)^{N_i - N_R} \frac{d}{dx} \left[\frac{\mu x}{\eta_i - \zeta_i x} \right] \\ &= \frac{\eta_i (\phi_{i,k} \mu)^{N_i - N_R + 1} x^{N_i - N_R} e^{-\frac{\mu \phi_{i,k} x}{\eta_i - \zeta_i x}}}{\Gamma(N_i - N_R + 1) (\eta_i - \zeta_i x)^{N_i - N_R + 2}}, \quad 0 \leq x < \frac{\eta_i}{\zeta_i}. \end{aligned} \quad (25)$$

By averaging over the respective PDFs, the sum rate over semi-correlated Rayleigh fading can now be derived as

$$\begin{aligned} \mathcal{C} &= \sum_{i=1}^2 \sum_{k=1}^{N_R} \int_0^{\infty} \frac{t^{N_i - N_R} e^{-t}}{2 \ln(2) \Gamma(N_i - N_R + 1)} \ln \left(\frac{\phi_{i,k} \mu + (\eta_i + \zeta_i) t}{\phi_{i,k} \mu + \zeta_i t} \right) dt \\ &= \frac{1}{2 \ln(2)} \sum_{i=1}^2 \sum_{k=1}^{N_R} [\mathbb{J}(a, b, c_1) - \mathbb{J}(a, b, c_2)], \end{aligned} \quad (26)$$

where $a = N_i - N_R$, $b = \phi_{i,k} \mu$, $c_1 = \eta_i + \zeta_i$, and $c_2 = \zeta_i$. In (26), the function $\mathbb{J}(a, b, c)$ is defined as

$$\mathbb{J}(a, b, c) \triangleq \frac{1}{\Gamma(a+1)} \int_0^{\infty} t^a e^{-t} \ln(b+ct) dt. \quad (27)$$

By first using the identity $t^a e^{-t} = -\frac{d}{dt} (\Gamma(a+1, t))$ and then employing partial integration of (27), $\mathbb{J}(a, b, c)$ can be simplified as

$$\mathbb{J}(a, b, c) = \ln(b) + \frac{c}{\Gamma(a+1)} \int_0^{\infty} \frac{\Gamma(a, t)}{b+ct} dt, \quad (28)$$

By using the identity [10, Eq. (8.352.2)], and then applying a change of variable, $s = b + ct$, (28) can be evaluated in closed-form by using [10, Eq. (3.351.2)] as in (12).

Next, the PDF of $\gamma_{S_i^{(k)}}$ for i.i.d. Rayleigh fading can readily be obtained by substituting $\phi_{i,k} = 1$ for $i \in \{1, 2\}$ and $k \in \{1, \dots, N_R\}$ into (25) as

$$f_{\gamma_{S_i^{(k)}}}(x) = \frac{\eta_i \mu^{N_i - N_R + 1} x^{N_i - N_R} e^{-\frac{\mu x}{\eta_i - \zeta_i x}}}{\Gamma(N_i - N_R + 1) (\eta_i - \zeta_i x)^{N_i - N_R + 2}}, \quad 0 \leq x < \frac{\eta_i}{\zeta_i}. \quad (29)$$

Now, by using similar steps to those in (26), (27) and (28), the sum rate over i.i.d. Rayleigh fading can be derived as given in (11).

APPENDIX II

Proof of the sum rate upper bound for doubly-correlated Rayleigh fading

In this Appendix, the proof of the upper bound of the sum rate over doubly-correlated Rayleigh fading is sketched. To this end, we recall the following identity [14]

$$\left[\left(\left(\mathbf{H}^{(i,R)} \right)^H \mathbf{H}^{(i,R)} \right)^{-1} \right]_{k,k} = \frac{\det \left(\left(\mathbf{H}_k^{(i,R)} \right)^H \mathbf{H}_k^{(i,R)} \right)}{\det \left(\left(\mathbf{H}^{(i,R)} \right)^H \mathbf{H}^{(i,R)} \right)}. \quad (30)$$

By substituting (30) into (10), the sum rate can be re-written as in (31). By applying Jensen's inequality, an upper bound of the sum rate can be derived as in (32). Next, we employ the following two recent results in random matrix theory [19] to evaluate (32) in closed-form.

$$\begin{aligned} & \mathcal{E} \left\{ \det \left(\left(\mathbf{H}^{(i,R)} \right)^H \mathbf{H}^{(i,R)} \right) \right\} \\ &= \det \left(\Psi^{(R,i)} \right) \mathcal{E} \left\{ \det \left(\left(\mathbf{H}^{(i)} \right)^H \Phi^{(i)} \mathbf{H}^{(i)} \right) \right\} \\ &= \frac{(N_R)! \det \left(\Psi^{(R,i)} \right) \det \left(\mathcal{A}^{(i)} \right)}{\prod_{p < q}^{N_i} \left(\tau_q^{(i)} - \tau_p^{(i)} \right)}, \end{aligned} \quad (33)$$

where $\mathcal{A}^{(i)}$ and $\tau_q^{(i)}$ are defined under (14). Similarly, by noticing the fact that $\mathbf{H}_k^{(i,R)} \sim \mathcal{CN}(\mathbf{0}_{N_i \times N_R - 1}, \Phi^{(i)} \otimes \Psi_{kk}^{(R,i)})$, (33) can be extended as [16]

$$\mathcal{E} \left\{ \det \left(\left(\mathbf{H}_k^{(i,R)} \right)^H \mathbf{H}_k^{(i,R)} \right) \right\} = \frac{(N_R - 1)! \det \left(\Psi_{kk}^{(R,i)} \right) \det \left(\mathcal{A}_{kk}^{(i)} \right)}{\prod_{p < q}^{N_i - 1} \left(\tau_{q,kk}^{(i)} - \tau_{p,kk}^{(i)} \right)}, \quad (34)$$

where $\mathcal{A}_{kk}^{(i)}$ and $\tau_{q,kk}^{(i)}$ are again defined under (14). Now, by substituting (33) and (34) into (32), and after some manipulations, the desired result can be derived as in (14).

$$\mathcal{C} = \frac{1}{2} \sum_{i=1}^2 \sum_{k=1}^{N_R} \mathcal{E} \left\{ \log_2 \left[(\zeta_i + \eta_i) \det \left(\left(\mathbf{H}^{(i,R)} \right)^H \mathbf{H}^{(i,R)} \right) + \mu \det \left(\left(\mathbf{H}_k^{(i,R)} \right)^H \mathbf{H}_k^{(i,R)} \right) \right] \right. \\ \left. - \log_2 \left[\zeta_i \det \left(\left(\mathbf{H}^{(i,R)} \right)^H \mathbf{H}^{(i,R)} \right) + \mu \det \left(\left(\mathbf{H}_k^{(i,R)} \right)^H \mathbf{H}_k^{(i,R)} \right) \right] \right\}. \quad (31)$$

$$\mathcal{C} \leq \mathcal{C}_{ub} = \frac{1}{2 \ln(2)} \sum_{i=1}^2 \sum_{k=1}^{N_R} \ln \left[\frac{(\zeta_i + \eta_i) \mathcal{E} \left\{ \det \left(\left(\mathbf{H}^{(i,R)} \right)^H \mathbf{H}^{(i,R)} \right) \right\} + \mu \mathcal{E} \left\{ \det \left(\left(\mathbf{H}_k^{(i,R)} \right)^H \mathbf{H}_k^{(i,R)} \right) \right\}}{\zeta_i \mathcal{E} \left\{ \det \left(\left(\mathbf{H}^{(i,R)} \right)^H \mathbf{H}^{(i,R)} \right) \right\} + \mu \mathcal{E} \left\{ \det \left(\left(\mathbf{H}_k^{(i,R)} \right)^H \mathbf{H}_k^{(i,R)} \right) \right\}} \right]. \quad (32)$$

$$\mathcal{C} = \frac{1}{2} \sum_{i=1}^2 \sum_{k=1}^{N_R} \mathcal{E} \left\{ \log_2 \left[1 + \eta_i \exp \left(\ln \left[\det \left(\left(\mathbf{H}^{(i,R)} \right)^H \mathbf{H}^{(i,R)} \right) \right] - \ln \left[\zeta_i \det \left(\left(\mathbf{H}^{(i,R)} \right)^H \mathbf{H}^{(i,R)} \right) + \mu \det \left(\left(\mathbf{H}_k^{(i,R)} \right)^H \mathbf{H}_k^{(i,R)} \right) \right] \right] \right\}. \quad (36)$$

$$\mathcal{C} \geq \mathcal{C}_{lb} = \frac{1}{2} \sum_{i=1}^2 \sum_{k=1}^{N_R} \log_2 \left[1 + \frac{\eta_i \exp \left(\mathcal{E} \left\{ \ln \left[\det \left(\left(\mathbf{H}^{(i,R)} \right)^H \mathbf{H}^{(i,R)} \right) \right] \right\} \right)}{\zeta_i \mathcal{E} \left\{ \det \left(\left(\mathbf{H}^{(i,R)} \right)^H \mathbf{H}^{(i,R)} \right) \right\} + \mu \mathcal{E} \left\{ \det \left(\left(\mathbf{H}_k^{(i,R)} \right)^H \mathbf{H}_k^{(i,R)} \right) \right\}} \right]. \quad (37)$$

APPENDIX III

Proof of the sum rate lower bound for doubly-correlated Rayleigh fading

In this Appendix, the proof of the lower bound of the sum rate over doubly-correlated fading is sketched. In this context, the sum rate in (10) can be re-written as [16], [20]

$$\mathcal{C} = \frac{1}{2} \sum_{i=1}^2 \sum_{k=1}^{N_R} \mathcal{E} \left\{ \log_2 \left[1 + \eta_i e^{\ln \left[1 / \left(\zeta_i + \mu \left(\left(\mathbf{H}^{(i,R)} \right)^H \mathbf{H}^{(i,R)} \right)^{-1} \right) \right]} \right] \right\}. \quad (35)$$

By substituting (30) into (35), the sum rate can further be expanded as given in (36). Next, by employing the Jensen's inequality [20], a lower bound for the sum rate can be derived as in (37). Again, (36) can be evaluated in closed-form by employing the following identity [19]

$$\mathcal{E} \left\{ \ln \left[\det \left(\left(\mathbf{H}^{(i,R)} \right)^H \mathbf{H}^{(i,R)} \right) \right] \right\} \\ = \sum_{l=1}^{N_R} \psi(l) + \frac{\sum_{l=N_i-N_R+1}^{N_i} \det \left(\mathcal{B}^{(i,k)} \right)}{\left(\prod_{p < q}^{N_i} \left(\tau_q^{(i)} - \tau_p^{(i)} \right) \right)}, \quad (38)$$

where $\mathcal{B}^{(i,k)}$ is defined under (17). Next, by substituting (33), (34) and (38) into (37), the sum rate lower bound can be derived as (17).

REFERENCES

- [1] B. Rankov and A. Wittneben, "Spectral efficient protocols for half-duplex fading relay channels," *IEEE J. Sel. Areas Commun.*, vol. 25, no. 2, pp. 379–389, Feb. 2007.
- [2] Y. Han *et al.*, "Performance bounds for two-way amplify-and-forward relaying," *IEEE Trans. Wireless Commun.*, vol. 8, pp. 432–439, 2009.
- [3] R. H. Y. Louie, Y. Li, and B. Vucetic, "Practical physical layer network coding for two-way relay channels: performance analysis and comparison," *IEEE Trans. Wireless Commun.*, vol. 9, pp. 764–777, 2010.
- [4] Z. Ding, T. Ratnarajah, and K. Leung, "On the study of network coded AF transmission protocol for wireless multiple access channels," *IEEE Trans. Wireless Commun.*, vol. 8, no. 1, pp. 118–123, Jan. 2009.
- [5] R. Zhang *et al.*, "Optimal beamforming for two-way multi-antenna relay channel with analogue network coding," *IEEE J. Sel. Areas Commun.*, vol. 27, no. 5, pp. 699–712, Jun. 2009.
- [6] C. Li, L. Yang, and W.-P. Zhu, "Two-way MIMO relay precoder design with channel state information," *IEEE Trans. Commun.*, vol. 58, no. 12, pp. 3358–3363, Dec. 2010.
- [7] A. Y. Panah and R. W. Heath, "MIMO two-way amplify-and-forward relaying with imperfect receiver CSI," *IEEE Trans. Veh. Technol.*, vol. 59, no. 9, pp. 4377–4387, Nov. 2010.
- [8] G. Amaraluriya, C. Tellambura, and M. Ardakani, "Performance analysis of zero-forcing for two-way MIMO AF relay networks," *IEEE Wireless Commun. Lett.*, vol. 1, no. 2, pp. 53–56, Apr. 2012.
- [9] K.-J. Lee and I. Lee, "Achievable rate regions for two-way MIMO AF multiple-relay channels," in *Proc. 73rd IEEE Veh. Technol. Conf. (VTC Spring)*, May 2011, pp. 1–5.
- [10] I. Gradshteyn and I. Ryzhik, *Table of integrals, Series, and Products*, 7th ed. Academic Press, 2007.
- [11] A. Paulraj, R. Nabar, and D. A. Gore, *Introduction to Space-Time Wireless Communications*. Cambridge Univ. Press, Cambridge, U.K., 2003.
- [12] J. Heath, R.W., S. Sandhu, and A. Paulraj, "Antenna selection for spatial multiplexing systems with linear receivers," *IEEE Commun. Lett.*, vol. 5, no. 4, pp. 142–144, Apr. 2001.
- [13] R. Louie, Y. Li, and B. Vucetic, "Zero forcing in general two-hop relay networks," *IEEE Trans. Veh. Technol.*, vol. 59, no. 1, pp. 191–202, Jan. 2010.
- [14] D. Gore, J. Heath, R.W., and A. Paulraj, "On performance of the zero forcing receiver in presence of transmit correlation," in *Proc. IEEE Int. Symp. Inf. Theory. (ISIT)*, 2002.
- [15] —, "Transmit selection in spatial multiplexing systems," *IEEE Commun. Lett.*, vol. 6, no. 11, pp. 491–493, Nov. 2002.
- [16] M. Matthaiou, C. Zhong, and T. Ratnarajah, "Novel generic bounds on the sum rate of MIMO ZF receivers," *IEEE Trans. Signal Process.*, vol. 59, no. 9, pp. 4341–4353, Sep. 2011.
- [17] H. Bolcskei, M. Borgmann, and A. J. Paulraj, "Impact of the propagation environment on the performance of space-frequency coded MIMO-OFDM," *IEEE J. Sel. Areas Commun.*, vol. 21, no. 3, pp. 427–439, Apr. 2003.
- [18] M. Abramowitz and I. Stegun, *Handbook of Mathematical Functions*. Dover Publications, Inc., New York, 1970.
- [19] S. Jin *et al.*, "Ergodic capacity analysis of amplify-and-forward MIMO dual-hop systems," *IEEE Trans. Inf. Theory*, vol. 56, no. 5, pp. 2204–2224, May 2010.
- [20] O. Oyman *et al.*, "Characterizing the statistical properties of mutual information in MIMO channels," *IEEE Trans. Signal Process.*, vol. 51, no. 11, pp. 2784–2795, Nov. 2003.